PAPER

SLNR-Based Joint Precoding for RIS Aided Beamspace HAP-NOMA Systems

Pingping JI[†a)], **Lingge JIANG**[†], **Chen HE**[†], **Di HE**[†], ***and*** **Zhuxian LIAN**[††], ***Nonmembers***

SUMMARY High altitude platform (HAP), known as line-of-sight dominated communications, effectively enhance the spectral efficiency of wireless networks. However, the line-of-sight links, particularly in urban areas, may be severely deteriorated due to the complex communication environment. The reconfigurable intelligent surface (RIS) is employed to establish the cascaded-link and improve the quality of communication service by smartly reflecting the signals received from HAP to users without direct-link. Motivated by this, the joint precoding scheme for a novel RIS-aided beamspace HAP with non-orthogonal multiple access (HAP-NOMA) system is investigated to maximize the minimum user signal-to-leakage-plus-noise ratio (SLNR) by considering user fairness. Specifically, the SLNR is utilized as metric to design the joint precoding algorithm for a lower complexity, because the isolation between the precoding obtainment and power allocation can make the two parts be attained iteratively. To deal with the formulated non-convex problem, we first derive the statistical upper bound on SLNR based on the random matrix theory in large scale antenna array. Then, the closed-form expressions of power matrix and passive precoding matrix are given by introducing auxiliary variables based on the derived upper bound on SLNR. The proposed joint precoding only depends on the statistical channel state information (SCSI) instead of instantaneous channel state information (ICSI). NOMA serves multi-users simultaneously in the same group to compensate for the loss of spectral efficiency resulted from the beamspace HAP. Numerical results show the effectiveness of the derived statistical upper bound on SLNR and the performance enhancement of the proposed joint precoding algorithm.
key words: *high altitude platform, signal-to-leakage-plus-noise ratio, reconfigurable intelligent surface, large scale array, non-orthogonal multiple access*

1. Introduction

Quasi-stationary high altitude platform (HAP), as a promising communication technology in beyond 5G/6G networks, is located at an altitude of 17–22 km to provide the stratospheric communication services with large coverage, long flight duration and quick deployment [1]. It is an indispensable component of air-space-ground integrated information communication network, i.e. satellite, stratosphere and terrestrial wireless networks. To date, some works have studied the integration of HAP and various wireless communication technologies to meet the explosive growth in the requirement of high data transmission rate and massive connectivity, such as multiple-input multiple-output (MIMO) [1], artificial intelligence [2], hybrid beamforming [3], non-orthogonal multiple access (NOMA) [4] and reconfigurable intelligent surface (RIS) [5].

Manuscript received March 22, 2024.
Manuscript publicized May 6, 2024.
[†]Shanghai Jiaotong University, China.
[††]Jiangsu University of Science and Technology, China.
a) E-mail: ji_pingping@sjtu.edu.cn
DOI: 10.23919/transcom.2024EBP3045

The introduction of NOMA to the beamspace HAP can tackle the issue of limited number of users by offering service for multi-users in the same time-frequency-space resource block, and improve the spectral efficiency (SE) by deploying superposition coding at the HAP and successive interference cancellation (SIC) at the terminal users [6]. The HAP realize NOMA in power domain other than time, frequency, or code domain, which can lengthen the endurance time of HAP by lowering the number of radio frequency and ensure the quality of service for HAP by allocating more power to users with poor conditions [4].

Recently, RIS has attracted worldwide attention from the academia and industry due to its characteristics of low cost and portability, which can be directly deployed in existing wireless networks without any other hardwares [7]–[11]. An RIS is a man-made electronmagnetic surface composed of a large number of programmable reconfigurable passive elements and a smart controller [7]. The controller adjusts the passive element, i.e. phase shift, by reflecting the incident signals to desired directions aiming at improving the communication service. In practice, it is prone to suffer severe path loss and serious signal blockage for the link between HAP and terrestrial users, and the RIS can overcome this by assisting the HAP to establish the cascaded-link, i.e. HAP-RIS-user link [5].

The key problem in RIS-aided communication systems is how to solve the joint precoding optimization problem, due to the non-convex objective functions and constraints. To maximize the sum rate in the form of a sum-of-log-ratio, some auxiliary variables has been introduced to derive the closed-form expressions of the passive precoding matrix at RIS and active precoding matrix at the base station [8]. However, each item in the reflecting matrix is highly related with the other items due to the utilization of production between vector and matrix, which incurs a lower complexity at the cost of SE. The first-order Taylor expansion has been used in [9] to transform the non-convex objective function into convex form, which result in performance loss. The maximization of the weighted sum rate has been solved by designing a joint transmit precoding and reflect precoding optimization scheme in [10]. The gradient-projection method has been utilized in the obtainment of the closed-form of passive and active beamforming matrices in [11]. The above works all focus on the instantaneous channel state information (ICSI), which is challenging to be acquired on HAP due to the large distance between HAP and users compared with the terrestrial systems.

The statistical channel state information (SCSI) has been utilized in [7] and [4]. The closed-form sum rate has been derived in a simple scenery which is not suitable in practice in [7] and the correlation of statistical correlation matrix has been analyzed. The mean-square-error has been researched to reformulate the non-convex ergodic sum rate objective into the convex form in [4] and the partial SCSI is used due to the digital precoder. Obviously, the feedback overhead, i.e. ICSI, becomes exponentially higher with the growth of the number of transmit antennas. Therefore, we design the schemes with SCSI [4] rather than ICSI [6] for the beamspace HAP-NOMA system.

It has been already shown in [9] and [4] that the computation of designing schemes in this downlink scenario is difficult with the signal-to-interference-plus-noise-ratio (SINR) criterion. The adopt of the signal-to-leakage-plus-noise-ratio (SLNR) criterion can reduce the computational complexity by iteratively designing the active beamforming and the power allocation as two disjoint subproblems [12].

In this paper, we study a downlink transmission algorithm for the RIS assisted beamspace HAP-NOMA systems according to SLNR. We aim to maximize the minimum SLNR of all users by jointly designing the passive precoding at the RIS and power allocation on HAP. The main contributions of this paper can be summarized as follows:

- A novel RIS-aided beamspace HAP-NOMA system is proposed. The NOMA combining beamspace HAP improves the achievable sum rate by improving the number of serving users simultaneously. The combination of RIS and beamspace HAP-NOMA makes the users without direct-link from HAP could achieve better service.
- The statistical upper bound on SLNR is derived according to the random matrix theory in large scale antenna. SLNR is used as performance measure for the RIS-aided HAP-NOMA system to reduce the computation complexity by decoupling the power allocation and passive precoding. The minimum SLNR is maximized to consider the user fairness.
- The closed form expressions of power allocation matrix and passive precoding matrix are obtained by introducing a series of auxiliary variables. To be specific, The Lagrange multiplier method is used to solve the power allocation problem, and the bisection method is used to solve the passive precoding problem.
- Numerical results show that the derived upper bound is effective and the proposed algorithm has an distinct performance enhancement.

The rest of this paper is organized as follows. Section 2 introduces the channel model for the novel RIS-aided beamspace HAP-NOMA system. Section 3 presents the main results, where a statistical upper bound on SLNR will be derived and a joint precoding algorithm will be proposed iteratively. Section 4 presents the simulation analysis and Sect. 5 concludes the paper.

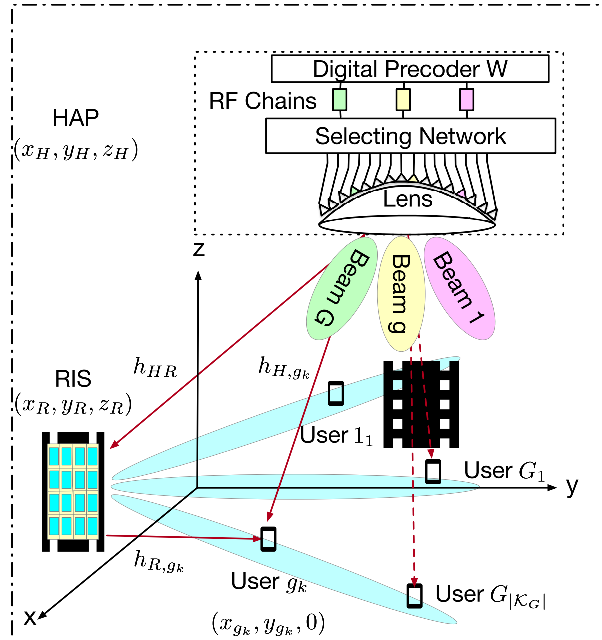

Fig. 1 System model of the proposed RIS-aided beamspace HAP-NOMA.

2. System Model

Consider a downlink RIS-aided beamspace HAP-NOMA system as shown in Fig. 1, where the HAP is equipped with a uniform planar antenna (UPA) of $M = M_v \times M_h$ transmit antennas and G RF chains. The K single-antenna users is served with the help of one RIS, which is equipped with $N = N_v \times N_h$ elements of UPA. The vertical and horizontal antenna spacing $d_0 = \lambda/2$ of RIS are same as that of HAP, λ is the carrier wavelength.

Denote the location of HAP, RIS and user k in group g as (x_H, y_H, z_H), (x_R, y_R, z_R) and $(x_{g_k}, y_{g_k}, 0)$. $\vartheta_{t,r} \in [0, \pi/2)$ and $\varphi_{t,r} \in [-\pi, \pi]$ are the vertical and horizontal angle of departure from transmitter to receiver, $\vartheta_{t,r} = \arctan(\sqrt{(x_t - x_r)^2 + (y_t - y_r)^2}/|z_t - z_r|)$ and $\varphi_{H,g_k} = \arccos((x_r - x_t)/\sqrt{(x_t - x_r)^2 + (y_t - y_r)^2}) \cdot \mathrm{sgn}(y_r - y_t)$, $\mathrm{sgn}(\cdot)$ is a sign function.

Denote the set of all users and the set of users in group g as $\mathcal{K}$ and $\mathcal{K}_g$ respectively. Denote the set of users with weak or no direct-link as $\mathcal{K}'$. Obviously, the number of groups is equal to the number of RF chains as G such that $|\mathcal{K}_g| \geq 1$, $\mathcal{K}_i \cap \mathcal{K}_j = \emptyset$ for $i \neq j$, $\sum_{g=1}^{G} |\mathcal{K}_g| = K$ and $\mathcal{K} = \bigcup_{g=1}^{G} \mathcal{K}_g$.

The user $\{k|k \in (\mathcal{K} - \mathcal{K}')\}$ with direct-link should be assigned to the beam b_{H,g_k} and the user $\{k|k \in \mathcal{K}'\}$ with weak or no direct-link should be in the beam b_{HR}, where $b_{t,r} = M_v(m_{t,r} - 1) + n_{t,r}$ with $m_{t,r} = \frac{M_v}{2} \sin\vartheta_{t,r} \cos\varphi_{t,r} + 1, \varphi_{t,r} \in [-\frac{\pi}{2}, \frac{\pi}{2}]$, $m_{t,r} = \frac{M_v}{2} \sin\vartheta_{t,r} \cos\varphi_{t,r} + M_v + 1, \varphi_{t,r} \notin [-\frac{\pi}{2}, \frac{\pi}{2}]$, $n_{t,r} = \frac{M_h}{2} \sin\vartheta_{t,r} \sin\varphi_{t,r} + 1, \varphi_{t,r} \in [0, \pi]$ and $n_{t,r} = \frac{M_h}{2} \sin\vartheta_{t,r} \sin\varphi_{t,r} + M_h + 1, \varphi_{t,r} \in [-\pi, 0)$ [4].

The NOMA with successive interference cancelation is utilized in the g-th group and the beamspace HAP-NOMA

Table 1 Definition of parameters used in Eq. (1).

x_{g_k}, y_{g_k}	g_kth transmitted and received signal, $\mathbb{E}[x_{g_k}x_{g_k}^H]=1$
$\vec{\mathbf{h}}_{g_k}$	g_kth $1\times G$ beamspace channel vector, $\vec{\mathbf{h}}_{g_k}=\mathbf{h}_{g_k}\mathbf{U}_s$
$\mathbf{h}_{g_k}$	g_kth $1\times M$ channel vector, $\mathbf{h}_{g_k}=\mathbf{h}_{H,g_k}+\mathbf{h}_{R,g_k}\mathbf{\Phi}\mathbf{h}_{HR}$
$\mathbf{h}_{H/R,g_k}$	channel vector from HAP/RIS to kth user in gth group
$\mathbf{h}_{HR}$	$N\times M$ channel matrix from HAP to RIS
$\mathbf{U}_s$	$M\times G$ selected beam matrix, $\mathbf{U}_s=\mathbf{U}(:,b)_{b\in\mathcal{B}}$
$\mathcal{B}$	the set of selected beams, $\lvert\mathcal{B}\rvert=G$
$\mathbf{w}_g$	gth $G\times 1$ digital precoding vector, $\lvert\mathbf{w}_g\rvert=1$
$\mathbf{\Phi}$	$N\times N$ diagonal phase shift matrix at RIS
p_{g_k}	g_kth transmitted power, $\sum_{j_i\in\mathcal{K}}p_{j_i}\le P$
P	total transmitted power
n	additive white Gaussian noise (AWGN), $\mathcal{CN}(0,\sigma^2)$
σ^2	noise variance

channels of users in g-th group satisfy $|\vec{\mathbf{h}}_{g_1}\mathbf{w}_g|^2\ge\cdots\ge|\vec{\mathbf{h}}_{g_{|\mathcal{K}_g|}}\mathbf{w}_g|^2$. The received signal at the kth user in gth group can be represented as [9]

$$\begin{aligned}y_{g_k}=&\underbrace{\vec{\mathbf{h}}_{g_k}\mathbf{w}_g\sqrt{p_{g_k}}x_{g_k}}_{\text{desired signal}}+\underbrace{\vec{\mathbf{h}}_{g_k}\mathbf{w}_g\sum_{i=1}^{k-1}\sqrt{p_{g_i}}x_{g_i}}_{\text{intra-beam interference}}\\&+\underbrace{\vec{\mathbf{h}}_{g_k}\sum_{j\neq g}\sum_{i=1}^{\mathcal{K}_j}\mathbf{w}_j\sqrt{p_{j_i}}x_{j_i}}_{\text{inter-beam interference}}+\underbrace{n_{g_k}}_{\text{noise}},\end{aligned}\tag{1}$$

where the parameters are defined in Table 1, $\mathbf{h}_{H/R,g_k}$ and $\mathbf{h}_{HR}$ are defined as [1]

$$\begin{aligned}\mathbf{h}_{H,g_k}=&\sqrt{\alpha_{H,g_k}\rho_{H,g_k}}\mathbf{a}(\vartheta_{H,g_k},\varphi_{H,g_k},M)+\\&\sqrt{\alpha_{H,g_k}(1-\rho_{H,g_k})}\mathbf{h}^w_{H,g_k}\widetilde{\mathbf{R}}^{1/2}_{H,g_k},\end{aligned}\tag{2a}$$

$$\begin{aligned}\mathbf{h}_{R,g_k}=&\sqrt{\alpha_{R,g_k}\rho_{R,g_k}}\mathbf{a}(\vartheta_{R,g_k},\varphi_{R,g_k},N)+\\&\sqrt{\alpha_{R,g_k}(1-\rho_{R,g_k})}\mathbf{h}^w_{R,g_k}\widetilde{\mathbf{R}}^{1/2}_{R,g_k},\end{aligned}\tag{2b}$$

$$\mathbf{h}_{HR}=\sqrt{\alpha_{HR}}\mathbf{a}(\vartheta_{RH},\varphi_{RH},N)^H\mathbf{a}(\vartheta_{HR},\varphi_{HR},M),\tag{2c}$$

$$\left[\widetilde{\mathbf{R}}_{t,r}\right]_{p,q}=\int_0^{\frac{\pi}{2}}\int_{-\pi}^{\pi}f(\varphi)f(\theta)e^{(j\frac{2\pi}{\lambda}(d_1+d_2))}d\varphi d\theta,\tag{2d}$$

where $f(\varphi)=\frac{e^{(\kappa_{t,r}\cos(\varphi-\mu_{t,r}))}}{2\pi I_0(\kappa)}$, $I_0(\cdot)$ is the zeroth-order modified Bessel function of first kind, $\mu_{t,r}\in[-\pi,\pi]$ is the horizontal AoD, $\kappa_{t,r}$ controls the angular spread (AS), $f(\theta)\propto e^{(-\sqrt{2}|\theta-\theta'_{t,r}|/\delta_{t,r})}$, $\theta'_{t,r}$ and $\delta_{t,r}$ are the mean vertical AoD and AS, $d_1=(p-q)d_0\sin\theta\cos\varphi$ and $d_2=(p-q)d_0\sin\theta\sin\varphi$.

Assume $\mathbf{U}=\mathbf{D}(M_v)\otimes\mathbf{D}(M_h)\in\mathbb{C}^{M\times M}$ is the spatial discrete Fourier transformation (DFT) matrix for 3D lens antenna array, where $\mathbf{D}(M)=\frac{1}{\sqrt{M}}[\mathbf{a}_M(0),\mathbf{a}_M(1/M),\cdots,\mathbf{a}_M((M-1)/M)]^H$ and $\mathbf{a}_M(x)=[1,e^{-j2\pi x},\cdots,e^{-j2\pi(M-1)x}]$,

$$\mathbf{a}(\vartheta,\varphi,N)=\mathbf{a}_{N_v}(\tfrac{d_0\sin\vartheta\cos\varphi}{\lambda})\otimes\mathbf{a}_{N_h}(\tfrac{d_0\sin\vartheta\sin\varphi}{\lambda}),\tag{3}$$

where $\rho_{t,r}=K_{t,r}/(1+K_{t,r})$, $K_{t,r}$ is the Rician factors, the large-scale fading fctor $\alpha_{t,r}=G_{t,r}(4\pi d_{t,r}/\lambda)^{-2}$ [1], $G_{t,r}$ is the effect of antenna gain from transmitter to receiver, $d_{t,r}$ is the distance between the transmitter and receiver. Finally, $\mathbf{h}^w_{H,g_k}\in\mathbb{C}^{1\times M}$ and $\mathbf{h}^w_{R,g_k}\in\mathbb{C}^{1\times N}$ are i.i.d. satisfying the complex Gaussian distribution $\mathcal{CN}(\mathbf{0},\mathbf{I})$.

We further define $\boldsymbol{\phi}=[\phi_1,\cdots,\phi_N]^H$, $c_{g_k}=\boldsymbol{\phi}^H\mathbf{c}_{g_k}$ and $\Xi_{g_k}=\boldsymbol{\phi}\mathbf{\Xi}_{g_k}\boldsymbol{\phi}^H$

$$\begin{aligned}\mathbf{c}_{g_k}=&\sqrt{\alpha_{HR}\alpha_{R,g_k}\rho_{R,g_k}}\\&\cdot\operatorname{diag}(\mathbf{a}(\vartheta_{R,g_k},\varphi_{R,g_k},N))\mathbf{a}(\vartheta_{RH},\varphi_{RH},N)^H,\end{aligned}\tag{4a}$$

$$\begin{aligned}\mathbf{\Xi}_{g_k}=&\alpha_{HR}\alpha_{R,g_k}(1-\rho_{R,g_k})\operatorname{diag}(\mathbf{a}(\vartheta_{RH},\varphi_{RH},N))\\&\widetilde{\mathbf{R}}_{R,g_k}\operatorname{diag}(\mathbf{a}(\vartheta_{RH},\varphi_{RH},N)^H).\end{aligned}\tag{4b}$$

The SLNR of the k-th user in g-th group is [12]

$$\mathrm{SLNR}_{g_k}=\frac{|\vec{\mathbf{h}}_{g_k}\mathbf{w}_g|^2p_{g_k}}{\sum_{j_i\in\mathcal{K}_{-g_k}}|\vec{\mathbf{h}}_{j_i}\mathbf{w}_g|^2p_{g_k}+\sigma^2},\tag{5}$$

where $\mathcal{K}_{-g_k}=(\bigcup_{j\neq g}\mathcal{K}_j)\bigcup\{g_1,\cdots,g_{k-1}\}$.

According to generalized eigenvalue decomposition [12] and equation (5), the optimum $\mathbf{w}_g=\frac{\mathbf{w}'_g}{|\mathbf{w}'_g|^2}$ with

$$\mathbf{w}'_g=(\sum_{j_i\in\mathcal{K}_{-g_1}}\vec{\mathbf{h}}^H_{j_i}\vec{\mathbf{h}}_{j_i}+\frac{\sigma^2}{p_{g_1}}\cdot\mathbf{I})^{-1}\vec{\mathbf{h}}^H_{g_1}.\tag{6}$$

3. Joint Precoding Scheme

In this section, we derive the upper bound of the SLNR. Then, the joint precoding algorithm is proposed to maximize the minimum user SLNR.

3.1 The Upper Bound on SLNR

We aim to maximize the SLNR only with the knowledge of SCSI. Assume $b_{HR}=G$ and $\mathcal{K}_{b_{HR}}=\mathcal{K}_G$. We derive the upper bound of SLNR in next theorem, which is proved in Appendix.

Theorem 1. *The upper bound of* SLNR_{g_k} *based on* (5) *can be further given as*

$$\mathrm{SLNR}^u_{g_k}=\frac{\delta'_{g,G}M\alpha_{H,g_k}\rho_{H,g_k}}{\frac{\sigma^2}{p_{g_k}}}+\frac{\delta_{g,G}(|\sqrt{\alpha_{H,g_k}\rho_{H,g_k}}+c_{g_k}|^2+\Xi_{g_k})+\delta'_{g,G}(c^H_{g_k}c_{g_k}+\Xi_{g_k})}{\sum\limits_{j_i\in\mathcal{K}_{-g_1}}(\frac{\Xi_{j_i}}{1+m_{j_i}}+\delta'_{j,G}c^H_{j_i}c_{j_i})+\eta+\frac{\sigma^2}{Mp_{g_k}}-\zeta_g},\tag{7}$$

where

$$\begin{aligned}\zeta_g=&\sum\nolimits_{l\neq g,G}\frac{\sum\limits_{n\in\mathcal{K}_l}\sqrt{\alpha_{H,l_n}\rho_{H,l_n}}c^H_{l_n}\sum\limits_{n\in\mathcal{K}_l}\sqrt{\alpha_{H,l_n}\rho_{H,l_n}}c_{l_n}}{\sum\limits_{n\in\mathcal{K}_l}\alpha_{H,l_n}\rho_{H,l_n}}\\=&\boldsymbol{\phi}^H\boldsymbol{\zeta}_g\boldsymbol{\phi},\end{aligned}\tag{8a}$$

$$\boldsymbol{\zeta}_g=\sum\nolimits_{l\neq g,G}\frac{\sum\limits_{n\in\mathcal{K}_l}\sqrt{\alpha_{H,l_n}\rho_{H,l_n}}\mathbf{c}^H_{l_n}\sum\limits_{n\in\mathcal{K}_l}\sqrt{\alpha_{H,l_n}\rho_{H,l_n}}\mathbf{c}_{l_n}}{\sum\limits_{n\in\mathcal{K}_l}\alpha_{H,l_n}\rho_{H,l_n}},\tag{8b}$$

$$\eta=\sum_{i=1}^{|\mathcal{K}_G|}|\sqrt{\alpha_{H,G_i}\rho_{H,G_i}}+c_{G_i}|^2,\tag{8c}$$

$$\begin{aligned}m_{g_k}=&\Xi_{g_k}/(\sum_{j_i\in\mathcal{K}_{-g_1}}(\frac{\Xi_{j_i}}{1+m_{j_i}}+\delta'_{j,G}c^H_{j_i}c_{j_i})\\&+\eta+\frac{\sigma^2}{Mp_{g_k}}-\zeta_g),\end{aligned}\tag{8d}$$

with the symbol m_{g_k} can be iteratively achieved by $m_{g_k} = \lim_{t\to\infty} m_{g_k}^{(t)}$ and $m_{g_k}^{(0)} = M$, and $\delta_{x,y}$ is a unit-impulse function, the value of which is zero when $x = y$ and one when $x \neq y$, $\delta'_{x,y} = 1 - \delta_{x,y}$.

3.2 Proposed Joint Precoding Scheme

The proposed joint precoding algorithm has been clarified in Algorithm 1. We obtain the $\mathbf{\Phi}, p_{g_k}$ closed-form optimal solution alternately by fixing the other variables.

Under the derivation of Theorem 1, the minimum user SLNR maximization problem can be formulated as

$$\begin{aligned}(\mathcal{P})\max_{p_{g_k},\mathbf{\Phi}}\ &\min\ \mathrm{SLNR}^{u}_{g_k}\\ s.t.\ C_1:\ &p_{g_k}\geq 0,\\ C_2:\ &\textstyle\sum_{g=1}^{G}\sum_{k=1}^{|\mathcal{K}_g|}p_{g_k}\leq P,\\ C_3:\ &|\theta_n|=1,\forall n,\end{aligned} \tag{9}$$

where C_1 ensures each user can be allocated with non-negative power, C_2 satisfies the maximum total power demand at the HAP, C_3 indicates the constraints of phase shift matrix $\mathbf{\Theta}$.

3.2.1 Algorithm for Optimizing p_{g_k} Given $\boldsymbol{\phi}$

By introducing auxiliary variable t, the problem $\mathcal{P}$ can be transformed as

$$\begin{aligned}&(\mathcal{P}_{p_{g_k}})\ \min_{\{p_{g_k}\}}\ t^{-1}\\ &s.t.\ C_1, C_2,\\ &C_4: t\leq \mathrm{SLNR}^{u}_{g_k} = A^{(1)}_{g_k}p_{g_k} + \frac{B^{(1)}_{g_k}}{C^{(1)}_{g_k}+\frac{\sigma^2}{p_{g_k}}}\end{aligned} \tag{10}$$

where

$$A^{(1)}_{g_k} = \delta'_{g,G}M\alpha_{H,g_k}\rho_{H,g_k}/\sigma^2, \tag{11a}$$

$$\begin{aligned}B^{(1)}_{g_k} &= \delta_{g,G}(|\sqrt{\alpha_{H,g_k}\rho_{H,g_k}} + c_{g_k}|^2 + \Xi_{g_k})\\ &+\delta'_{g,G}(c^{H}_{g_k}c_{g_k} + \Xi_{g_k}),\end{aligned} \tag{11b}$$

$$C^{(1)}_{g_k} = \sum_{j_i\in\mathcal{K}_{-g_1}}\left(\frac{\Xi_{j_i}}{1+m_{j_i}} + \delta'_{j,G}c^{H}_{j_i}c_{j_i}\right) + \eta - \zeta_g. \tag{11c}$$

Problem $\mathcal{P}_{p_{g_k}}$ is non-convex resulted from the multi-variable coupling in C_4, another auxiliary variables $\{b_{g_k}\}$ is introduced to make it solvable. And the problem $\mathcal{P}_{p_{g_k}}$ can be equivalently reformulated as

$$\begin{aligned}&(\mathcal{P}'_{p_{g_k}})\ \min_{\{p_{g_k}\}}\ t^{-1}\\ &s.t.\ C_1, C_2,\\ &C^{(1)}_4: A^{(1)}_{g_k}C^{(1)}_{g_k}p^2_{g_k} + (A^{(1)}_{g_k}\sigma^2 + B^{(1)}_{g_k})p_{g_k}\\ &\qquad\geq C^{(1)}_{g_k}b_{g_k} + \sigma^2 t,\\ &C^{(2)}_4: \begin{bmatrix} t, & \sqrt{b_{g_k}}\\ \sqrt{b_{g_k}}, & p_{g_k}\end{bmatrix}\geq 0,\\ &C^{(3)}_4: t\geq 0.\end{aligned} \tag{12}$$

The Lagrangian function of $(\mathcal{P}'_{p_{g_k}})$ is

$$\begin{aligned}&L(p_{g_k}, t, \boldsymbol{b}, \mu, \boldsymbol{\tau}, \boldsymbol{\kappa})\\ &= t^{-1} + \mu\left(\textstyle\sum_{g=1}^{G}\sum_{k=1}^{|\mathcal{K}_g|}p_{g_k} - P\right)\\ &+ \textstyle\sum_{g=1}^{G}\sum_{k=1}^{|\mathcal{K}_g|}\tau_{g_k}(C^{(1)}_{g_k}b_{g_k} + \sigma^2 t - A^{(1)}_{g_k}C^{(1)}_{g_k}p^2_{g_k}\\ &\qquad + (A^{(1)}_{g_k}\sigma^2 + B^{(1)}_{g_k})p_{g_k})\\ &+ \textstyle\sum_{g=1}^{G}\sum_{k=1}^{|\mathcal{K}_g|}\kappa_{g_k}(t - b_{g_k}p_{g_k}),\end{aligned} \tag{13}$$

where μ, $\boldsymbol{\tau}$ and $\boldsymbol{\kappa}$ are the Lagrange multipliers of C_2, $C^{(1)}_4$ and $C^{(2)}_4$ respectively. Therefore, the optimal p_{g_k} is [15]

$$p^{opt}_{g_k} = \frac{\mu + \tau_{g_k}(A^{(1)}_{g_k}\sigma^2 + B^{(1)}_{g_k}) - \kappa_{g_k}b_{g_k}}{2\tau_{g_k}A^{(1)}_{g_k}C^{(1)}_{g_k}}. \tag{14}$$

3.2.2 Algorithm for Optimizing $\mathbf{\Phi}$ Given p_{g_k}

We use the sub-multiplicativity of norm $\|\mathbf{AB}\| \leq \|\mathbf{A}\|\|\mathbf{B}\|$ and transform the item as $\sqrt{\alpha_{H,g_k}\rho_{H,g_k}}c_{g_k} \leq (\alpha_{H,g_k}\rho_{H,g_k}\|\boldsymbol{c}_{g_k}\|)(\boldsymbol{\phi}\boldsymbol{\phi}^H)$, then

$$\begin{aligned}\mathrm{SLNR}^{u}_{g_k} \leq &\frac{\mathrm{Tr}(\mathbf{A}_{g_k}\boldsymbol{\phi}\boldsymbol{\phi}^H + B_{g_k})}{\mathrm{Tr}(\mathbf{C}_{g_k}\boldsymbol{\phi}\boldsymbol{\phi}^H + D_{g_k})}\\ &+\frac{\delta'_{g,G}\alpha_{H,g_k}\rho_{H,g_k}}{\frac{\sigma^2}{Mp_{g_k}}},\end{aligned} \tag{15}$$

where

$$\mathbf{A}_{g_k} = (\boldsymbol{c}_{g_k}\boldsymbol{c}^H_{g_k} + \mathbf{\Xi}_{g_k} + \delta_{g,G}2\alpha_{H,g_k}\rho_{H,g_k}\|\boldsymbol{c}_{g_k}\|)\mathbf{I}), \tag{16a}$$

$$B_{g_k} = \delta_{g,G}\alpha_{H,g_k}\rho_{H,g_k}, \tag{16b}$$

$$\mathbf{C}_{g_k} = \sum_{j_i\in\mathcal{K}_{-g_1}}\left(\frac{\mathbf{\Xi}_{j_i}}{1+m_{j_i}} + \delta'_{j,G}\boldsymbol{c}_{j_i}\boldsymbol{c}^H_{j_i}\right) + \sum_{i=1}^{|\mathcal{K}_G|}\boldsymbol{c}_{G_i}\boldsymbol{c}^H_{G_i} - \boldsymbol{\zeta}_g, \tag{16c}$$

$$D_{g_k} = \frac{\sigma^2}{Mp_{g_k}} + \sum_{i=1}^{|\mathcal{K}_G|}\alpha_{H,G_i}\rho_{H,G_i}. \tag{16d}$$

By introducing two auxiliary variables t_1 and $\mathbf{Z} = \boldsymbol{\phi}\boldsymbol{\phi}^H$, and globally relaxing the feasible set of $\mathbf{Z}$ to its convex hull as $\{\mathbf{Z}|\mathrm{Tr}(\mathbf{Z}) = N, \mathbf{0}\leq\mathbf{Z}\leq\mathbf{I}\}$ [14]. The $\mathcal{P}$ is reformulated as

$$\begin{aligned}&(\mathcal{P}_{\boldsymbol{\phi}})\ \max_{\mathbf{Z}}\ t_1\\ &s.t.\ C_3,\\ &C_5: \mathrm{Tr}(\mathbf{A}_{g_k}\mathbf{Z} + B_{g_k})/\mathrm{Tr}(\mathbf{C}_{g_k}\mathbf{Z} + D_{g_k})\geq t_1,\\ &C_6: \mathrm{Tr}(\mathbf{Z}) = N,\\ &C_7: \mathbf{0}\leq\mathbf{Z}\leq\mathbf{I}.\end{aligned} \tag{17}$$

The problem $\mathcal{P}_{\boldsymbol{\phi}}$ is convex when t_1 is fixed. The bisection search method [14] can be utilized by setting

$$t_u = [(\lambda^{\max}_{\mathbf{A}_{g_k}} + B_{g_k})/(\lambda^{\min}_{\mathbf{C}_{g_k}} + D_{g_k})]^{\max}_{g,k}, \tag{18a}$$

$$t_l = [(\lambda^{\min}_{\mathbf{A}_{g_k}} + B_{g_k})/(\lambda^{\max}_{\mathbf{C}_{g_k}} + D_{g_k})]^{\min}_{g,k}, \tag{18b}$$

where $\lambda^{\max/\min}_{\mathbf{A}}$ is the maximum or minimum eigenvalue of matrix $\mathbf{A}$.

Given $\hat{t}\in\mathbb{R}$, the feasible Semi-Definite Programming problem $\mathcal{P}'_{\boldsymbol{\phi}}$ means $\hat{t}$ is a feasible solution of $\mathcal{P}_{\boldsymbol{\phi}}$, then the

Algorithm 1 Proposed Joint Precoding algorithm

```
Input: System parameters and SCSI.
1: Initialization: t = 1, p_{g_k}^0 and Φ^0. The maximum iterative number is
   set as T. The preset threshold ξ_t.
2: while t ≤ T do
3:    Obtain the optimal p_{g_k} by (14).
4:    Calculate t_u and t_l by (18).
5:    while t_u − t_l > ξ_t do
6:       t_1 = (t_l + t_u)/2.
7:       Solve P'_Φ with t_1 to check the feasibility of problem P'_Φ.
8:       if P'_Φ is feasible then
9:          Obtain Z_opt and Φ_opt by (19) and (20).
10:         t_l = t_1.
11:      else
12:         t_u = t_1.
13:      end if
14:   end while
15:   t = t + 1.
16: end while
Output: Φ and p_{g_k}, ∀g, k.
```

optimal solution of $\mathcal{P}_{\boldsymbol{\phi}}$ is in the interval of $[\hat{t}, t_u]$. Otherwise, the infeasible SDP problem $\mathcal{P}'_{\boldsymbol{\phi}}$ means the optimal solution of $\mathcal{P}_{\boldsymbol{\phi}}$ is in the interval of $[t_l, \hat{t}]$.

A recursive algorithm is designed from the step 5 to step 14 in Algorithm 1 to find out the optimal solution of $\mathcal{P}_{\boldsymbol{\phi}}$ by gradually narrowing down the feasible interval. Firstly, the initial value of t_1 is given as $(t_l + t_u)/2$, where t_l and t_u are denoted in (18). Next, the feasibility of $\mathcal{P}_{\boldsymbol{\phi}}$ is checked. If it is feasible, t_l is updated as t_1; otherwise, t_u is updated as t_1. Repeat the above steps until $t_u - t_l \leq \xi_t$, where ξ_t is the preset threshold [16].

With given t_1, the problem $\mathcal{P}_{\boldsymbol{\phi}}$ can be transformed as

$$
\begin{aligned}
&(\mathcal{P}'_{\boldsymbol{\phi}}) \text{ find } \mathbf{Z} \\
&s.t. \;\; C_3, C_5, C_6, C_7.
\end{aligned} \tag{19}
$$

Numerical program solvers can be used to solve the convex problem $\mathcal{P}'_{\boldsymbol{\phi}}$, and we can obtain the optimal $\mathbf{Z}_{opt}$. We then construct $\boldsymbol{\Phi}_{opt}$ based on $\boldsymbol{v}_1$, where $\boldsymbol{v}_1$ is the eigenvector corresponding to the largest eigenvalues of $\mathbf{Z}_{opt}$, as

$$
\boldsymbol{\Phi}_{opt} = \mathrm{diag}(\exp(j \arg(\boldsymbol{v}_1))). \tag{20}
$$

3.2.3 Complexity Analysis

In each iteration, μ, $\boldsymbol{\tau}$ and $\boldsymbol{\kappa}$ in (13) can be attained with the complexity $O(K^2 \log_2(\delta))$ [15], where δ is denoted as the preset accuracy. The complexity of the obtainment of t_u and t_l in (18) is $O(N^3)$. The worst case to obtain $\mathbf{Z}_{opt}$ and $\boldsymbol{\Phi}_{opt}$ has $\log_2((t_u - t_l)/\xi_t)$ iterations [14] with the complexity of $O(N^4 + N^2K)$ in each iteration [17]. The main complexity of the proposed joint precoding algorithm is

$$
\begin{aligned}
C_{pro} = O\{T[&(N^4 + N^2K)\log_2((t_u - t_l)/\xi_t) \\
&+ K^2 \log_2(\delta)]\}.
\end{aligned} \tag{21}
$$

The main complexity in [9] is

$$
\begin{aligned}
C_1 = O\{T[&\max(3K + 1 + G, KG)^4 \times \sqrt{KG}\log(\tfrac{1}{\xi}) \\
&+ (3K + N + 1)^4\sqrt{N+1}\log(\tfrac{1}{\xi}) \\
&+ (3K + N + 2)^4\sqrt{N+1}\log(\tfrac{1}{\xi})]\},
\end{aligned} \tag{22}
$$

where ξ is the required accuracy in [9].

The main complexity in [4] is

$$
C_2 = O\{T[K^2 \log_2(\delta)]\}, \tag{23}
$$

where δ is the required accuracy in [4].

Obviously, the complexity C_2 in (23) of [4] is the lowest as seen from (21)–(23). The second term in (21) is too small that it can be neglected. The t_u and t_l in (21) are defined in (16) and (18). Due to the large-scale fading on HAP, the t_u and t_l are 10^{-5} and 10^{-15} approximately by 10^3 times of repetitive simulations. The value of $\log_2((t_u - t_l)/\xi_t)$ is approximately equal to $\log(\frac{1}{\xi})$, and the value of $N^4 + N^2K \approx N^4$ because the number of antennas N is too larger than the number of users K in this paper. Finally, we can get that $C_2 < C_{pro} < C_1$.

4. Numerical Results and Analysis

In this section, the performance of the proposed algorithm is evaluated. The simulation parameters of variables for RIS-aided HAP-NOMA system are shown in Table 2 based on [1].

As shown in Fig. 2, we analyze the trends of the sum SLNR of the users $\sum_{g=1}^{G}\sum_{k=1}^{|\mathcal{K}_g|} \mathrm{SLNR}_{g_k}$ with respect to the total transmitted power P. In this simulation, we set $M = 256$. Figure 2 proves the effectiveness of the closed-form expressions which we deduced for the upper bound on SLNR in (7) for the RIS-aided HAP-NOMA systems. The Monte-carlo simulations depicts the $\sum_{g=1}^{G}\sum_{k=1}^{|\mathcal{K}_g|} \mathrm{SLNR}^u_{g_k}$ with respect to P, where $\mathrm{SLNR}^u_{g_k}$ is

Table 2 Simulation parameters.

Variables	Simulation Parameters
Location of HAP	$(x_H, y_H, z_H) = (0, 0, 2 \times 10^4)$
Location of RIS	$(x_R, y_R, z_R) = (0, 5 \times 10^3, 40)$
Frequency	2.4GHz
Bandwidth	10MHz
Noise variance	$\sigma^2 = -80$dBm
Number of antennas on HAP	$M_v = M_h$
Number of antennas on RIS	$N_v = N_h = 8$
Number of users	$K = 20$
Number of no direct-link users	$\lvert\mathcal{K}'\rvert = 10$
Radius of circle, K users randomly distributed	2×10^4
Radius of circle, $\mathcal{K}'$ users randomly distributed	30
Variables in (2d)	$\kappa_{t,r} = 5$, $\mu_{t,r} = 0°$, $\theta'_{t,r} = 30°$, $\delta_{t,r} = 10°$
Antenna Gain	$G_{H,g_k} = G_{R,g_k} = 0.5$, $G_{HR} = 1.45$
Iterative number	$T = 20$
Preset threshold	$\xi_t = 10^{-6}$

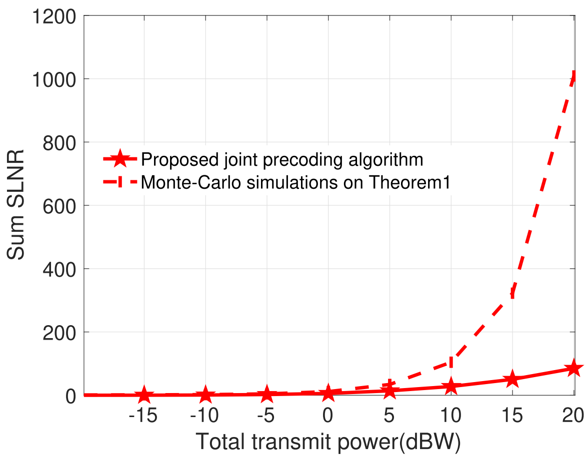

Fig. 2 Sum SLNR versus total transmit power. $M = 256$.

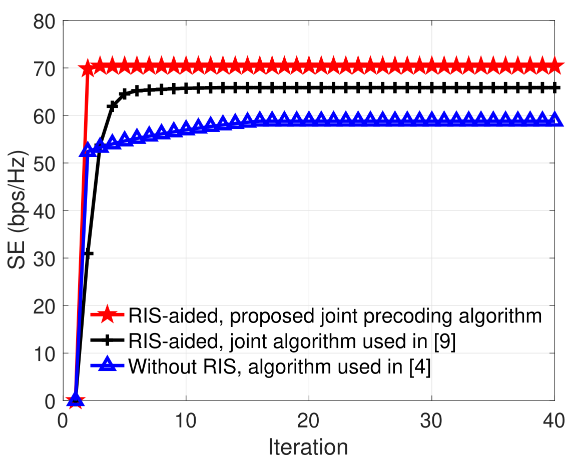

Fig. 3 SE versus iteration. $M = 256$ and $P = 20$ dBW.

defined in (7). And the proposed joint precoding algorithm depicts the $\sum_{g=1}^{G}\sum_{k=1}^{|\mathcal{K}_g|}\text{SLNR}_{g_k}$ with respect to P, where SLNR_{g_k} is defined in (5).

As shown in Fig. 3, the SE performance of the proposed scheme has been evaluated. In this simulation, we set $M = 256$ and $P = 20$dBW. For comparison, we plot the SE achieved by joint algorithm in [9] and without RIS algorithm in [4]. The proposed algorithm outperforms the algorithm in [9] due to the performance loss of the utilization of first-order Taylor expansion in [9]. The worst performance of the algorithm in [4] is because the RIS have not been used. The convergence speed of the proposed algorithm is faster than the other two algorithms due to the closed-form expression on upper bound of SLNR.

Figure 4 shows the SE performance of the proposed scheme with respect to total transmitted power P and the number of antennas on HAP M. As we can observe, the SE obtained by all these algorithms increase with the growth of P and M. In terms of SE, the proposed algorithm with RIS outperforms the other two algorithms, owing to the same reason as mentioned.

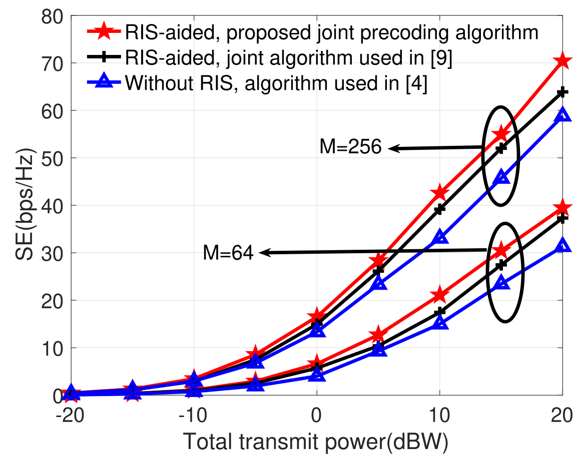

Fig. 4 SE versus total transmit power with respect to different number of antennas M on HAP.

5. Conclusion

In this paper, we have studied a downlink transmission algorithm for the RIS assisted beamspace HAP-NOMA systems according to SLNR. We have aimed to maximize the minimum SLNR of all users by jointly designing the passive precoding at the RIS and power allocation on HAP. The main contributions of this paper could be summarized as follows:

- A novel RIS-aided beamspace HAP-NOMA system has been proposed. The NOMA combining beamspace HAP has improved the achievable sum rate by improving the number of serving users simultaneously. The combination of RIS and beamspace HAP-NOMA has made the users without direct-link from HAP could achieve better service.
- The statistical upper bound on SLNR has been derived according to the random matrix theory in large scale antenna. SLNR has been used as performance measure for the RIS-aided HAP-NOMA system to reduce the computation complexity by decoupling the power allocation and passive precoding. The minimum SLNR has been maximized to consider the user fairness.
- The closed form expressions of power allocation matrix and passive precoding matrix have been obtained by introducing a series of auxiliary variables. To be specific, The Lagrange multiplier method has been used to solve the power allocation problem, and the bisection method has been used to solve the passive precoding problem.
- Numerical results have shown that the derived upper bound is effective and the proposed algorithm has an distinct performance enhancement.

References

[1] Z. Lian, Y. Su, Y. Wang, and L. Jiang, "A non-stationary 3-D wideband channel model for intelligent reflecting surface-assisted HAP-MIMO communication systems," IEEE Trans. Veh. Technol., vol.71,

no.2, pp.1109–1123, Feb. 2022.

[2] M. Guan, Z. Wu, Y. Cui, X. Cao, L. Wang, J. Ye, and B. Peng, "Efficiency evaluations based on artificial intelligence for 5G massive MIMO communication systems on high-altitude platform stations," IEEE Trans. Ind. Informat., vol.16, no.10, pp.6632–6640, Oct. 2020.

[3] Z. Lian, L. Jiang, C. He, and D. He, "User grouping and beamforming for HAP massive MIMO systems based on statistical-eigenmode," IEEE Wireless Commun. Lett., vol.8, no.3, pp.961–964, June 2019.

[4] P. Ji, L. Jiang, C. He, Z. Lian, and D. He, "Energy-efficient beamforming for beamspace HAP-NOMA systems," IEEE Commun. Lett., vol.25, no.5, pp.1678–1681, May 2021.

[5] N. Gao, S. Jin, X. Li, and M. Matthaiou, "Aerial RIS-assisted high altitude platform communications," IEEE Wireless Commun, Lett., vol.10, no.10, pp.2096–2100, Oct. 2021.

[6] B. Wang, L. Dai, Z. Wang, N. Ge, and S. Zhou, "Spectrum and energy-efficient beamspace MIMO-NOMA for millimeter-wave communications using lens antenna array," IEEE J. Sel. Areas Commun., vol.35, no.10, pp.2370–2382, Oct. 2017.

[7] J. Wang, H. Wang, Y. Han, S. Jin, and X. Li, "Joint transmit beamforming and phase shift design for reconfigurable intelligent surface assisted MIMO systems," IEEE Trans. Cogn. Commun. Netw., vol.7, no.2, pp.354–368, June 2021.

[8] X. Ma, S. Guo, H. Zhang, Y. Fang, and D. Yuan, "Joint beamforming and reflecting design in reconfigurable intelligent surface-aided multi-user communication systems," IEEE Trans. Wireless Commun., vol.20, no.5, pp.3269–3283, May 2021.

[9] P. Liu, Y. Li, W. Cheng, X. Gao, and X. Huang, "Intelligent reflecting surface sided NOMA for millimeter-wave massive MIMO with lens antenna array," IEEE Trans. Veh. Technol., vol.70, no.5, pp.4419–4434, May 2021.

[10] H. Guo, Y. Liang, J. Chen, and E.G. Larsson, "Weighted sum-rate maximization for reconfigurable intelligent surface aided wireless networks," IEEE Trans. Wireless Commun., vol.19, no.5, pp.3064–3076, May 2020.

[11] C. Pradhan, A. Li, L. Song, B. Vucetic, and Y. Li, "Hybrid precoding design for reconfigurable intelligent surface aided mmWave communication systems," IEEE Wireless Commun. Lett., vol.9, no.7, pp.1041–1045, July 2020.

[12] L. Pang, W. Wu, Y. Zhang, Y. Yuan, Y. Chen, A. Wang, and J. Li, "Joint power allocation and hybrid beamforming for downlink mmWave-NOMA systems," IEEE Trans. Veh. Technol., vol.70, no.10, pp.10173–10184, Oct. 2021.

[13] S. Wagner, R. Couillet, M. Debbah, and D.T.M. Slock, "Large system analysis of linear precoding in correlated MISO broadcast channels under limited feedback," IEEE Trans. Inf. Theory, vol.58, no.7, pp.4509–4537, July 2012.

[14] B. Su, X. Ding, C. Liu, and Y. Wu, "Heteroscedastic max–min distance analysis for dimensionality reduction," IEEE Trans. Image Process., vol.27, no.8, pp.4052–4065, Aug. 2018.

[15] S. Boyd and L. Vandenberghe, Convex Optimization. Cambridge, Cambridge Univ. Press, U.K., 2004.

[16] C. Shen, H. Li, and M. Brooks, "Supervised dimensionality reduction via sequential semidefinite programming," Pattern Recognition, vol.41, no.12, pp.3644–3652, 2008.

[17] K.-Y. Wang, A.M.-C. So, T.-H. Chang, W.-K. Ma, and C.-Y. Chi, "Outage constrained robust transmit optimization for multiuser MISO downlinks: Tractable approximations by conic optimization," IEEE Trans. Signal Process., vol.62, no.21, pp.5690–5705, Nov. 2014.

Appendix: Proof of Theorem 1

We derive Theorem 1 by setting some temporary variables $\mathbf{F}_{g_k} = (\sum_{j_i \in \mathcal{K}_{-g_k}} \vec{\mathbf{h}}_{j_i}^H \vec{\mathbf{h}}_{j_i} + \frac{\sigma^2}{p_{g_k}} \mathbf{I})^{-1}$, $\widetilde{\mathbf{w}}_g = \mathbf{F}_{g_1} \vec{\mathbf{h}}_{g_1}^H$ and

$$\upsilon_{g_k} = \frac{\widetilde{\mathbf{w}}_g^H \vec{\mathbf{h}}_{g_k}^H \vec{\mathbf{h}}_{g_k} \widetilde{\mathbf{w}}_g}{\widetilde{\mathbf{w}}_g^H (\sum_{j_i \in \mathcal{K}_{-g_{k+1}}} \vec{\mathbf{h}}_{j_i}^H \vec{\mathbf{h}}_{j_i} + \frac{\sigma^2}{p_{g_k}} \mathbf{I}) \widetilde{\mathbf{w}}_g}. \tag{A· 1}$$

Let $\mathbf{g}_{g_k} = \frac{1}{\sqrt{M}} \mathbf{h}_{H,g_k}^w \sim \mathcal{CN}(\mathbf{0}, \frac{1}{M}\mathbf{I})$, $\mathbf{l}_{g_k} = \frac{1}{\sqrt{N}} \mathbf{h}_{R,g_k}^w \sim \mathcal{CN}(\mathbf{0}, \frac{1}{N}\mathbf{I})$, $\hat{\vec{\mathbf{h}}}_{g_k} = \sqrt{\alpha_{H,g_k} \rho_{H,g_k}} \mathbf{a}(\vartheta_{H,g_k}, \varphi_{H,g_k}, M) + \sqrt{\alpha_{R,g_k} \rho_{R,g_k}} \mathbf{a}(\vartheta_{R,g_k}, \varphi_{R,g_k}, N) \mathbf{\Phi} \mathbf{h}_{HR}$ and $\tilde{\vec{\mathbf{h}}}_{g_k} = \sqrt{\alpha_{H,g_k}(1-\rho_{H,g_k})} \mathbf{h}_{H,g_k}^w \widetilde{\mathbf{R}}_{H,g_k}^{1/2} + \sqrt{\alpha_{R,g_k}(1-\rho_{R,g_k})} \mathbf{h}_{R,g_k}^w \widetilde{\mathbf{R}}_{R,g_k}^{1/2} \mathbf{\Phi} \mathbf{h}_{HR}$. We use (2) to get

$$\begin{aligned}
&\vec{\mathbf{h}}_{g_k} \mathbf{F}_{g_k} \vec{\mathbf{h}}_{g_k}^H \\
&= \hat{\vec{\mathbf{h}}}_{g_k} \mathbf{F}_{g_k} \hat{\vec{\mathbf{h}}}_{g_k}^H + \hat{\vec{\mathbf{h}}}_{g_k} \mathbf{F}_{g_k} \tilde{\vec{\mathbf{h}}}_{g_k}^H + \tilde{\vec{\mathbf{h}}}_{g_k} \mathbf{F}_{g_k} \hat{\vec{\mathbf{h}}}_{g_k}^H + \tilde{\vec{\mathbf{h}}}_{g_k} \mathbf{F}_{g_k} \tilde{\vec{\mathbf{h}}}_{g_k}^H \\
&\overset{(a)}{=} \hat{\vec{\mathbf{h}}}_{g_k} \mathbf{F}_{g_k} \hat{\vec{\mathbf{h}}}_{g_k}^H \\
&+M(\alpha_{H,g_k}(1-\rho_{H,g_k})) \mathbf{g}_{g_k} \widetilde{\mathbf{R}}_{H,g_k}^{1/2} \mathbf{U}_s \mathbf{F}_{g_k} \mathbf{U}_s^H \widetilde{\mathbf{R}}_{H,g_k}^{1/2} \mathbf{g}_{g_k}^H \\
&+N \mathbf{l}_{g_k} \mathbf{\Xi}_{g_k}^{\frac{1}{2}} \boldsymbol{\phi}^H \mathbf{a}(\vartheta_{HR}, \varphi_{HR}, M) \mathbf{U}_s \mathbf{F}_{g_k} \mathbf{U}_s^H \\
&\cdot \mathbf{b}(\vartheta_{HR}, \varphi_{HR}, M)^H \boldsymbol{\phi} \mathbf{\Xi}_{g_k}^{\frac{1}{2}} \mathbf{l}_{g_k}^H \\
&\overset{(b)}{=} \mathrm{Tr}(\hat{\vec{\mathbf{h}}}_{g_k}^H \hat{\vec{\mathbf{h}}}_{g_k} \mathbf{F}_{g_k} \\
&+(\alpha_{H,g_k}(1-\rho_{H,g_k})) \mathbf{U}_s^H \widetilde{\mathbf{R}}_{H,g_k} \mathbf{U}_s \mathbf{F}_{g_k} \\
&+\Xi_{g_k} \mathbf{U}_s^H \mathbf{a}(\vartheta_{HR}, \varphi_{HR}, M)^H \mathbf{a}(\vartheta_{HR}, \varphi_{HR}, M) \mathbf{U}_s \mathbf{F}_{g_k}) \\
&\overset{(c)}{=} \mathrm{Tr}(\vec{\mathbf{R}}_{g_k,g_k} \mathbf{F}_{g_k})
\end{aligned} \tag{A· 2}$$

where (a) follows from the Lemma 5 in [13], (b) follows from the Lemma 4 in [13] and (c) follows from the Theorem 1 in [4] and

$$\begin{aligned}
\vec{\mathbf{R}}_{g_k,g_k} &= M(\sqrt{\alpha_{H,g_k} \rho_{H,g_k}} \lambda_G^g + c_{g_k} \lambda_G^G)^H \\
&\cdot (\sqrt{\alpha_{H,g_k} \rho_{H,g_k}} \lambda_G^g + c_{g_k} \lambda_G^G) \\
&+M \Xi_{g_k} \mathbf{\Lambda}_M^{(G,G)}.
\end{aligned} \tag{A· 3}$$

We utilize $(A.1)$, $(A.2)$ and $(A.3)$ to get SLNR_{g_k} as

$$\begin{aligned}
&\mathrm{SLNR}_{g_k} \\
&= \frac{\vec{\mathbf{h}}_{g_1} \mathbf{F}_{g_1} \vec{\mathbf{h}}_{g_k}^H \vec{\mathbf{h}}_{g_k} \mathbf{F}_{g_1} \vec{\mathbf{h}}_{g_1}^H}{(\sum_{j_i \in \mathcal{K}_{-g_k}} \vec{\mathbf{h}}_{g_1} \mathbf{F}_{g_1} \vec{\mathbf{h}}_{j_i}^H \vec{\mathbf{h}}_{j_i} \mathbf{W}_{g_1} \vec{\mathbf{h}}_{g_1}^H + \frac{\sigma^2}{p_{g_k}} \vec{\mathbf{h}}_{g_1} \mathbf{F}_{g_1}^2 \vec{\mathbf{h}}_{g_1}^H)} \\
&= \frac{\vec{\mathbf{h}}_{g_1} \mathbf{F}_{g_1} \vec{\mathbf{h}}_{g_k}^H \vec{\mathbf{h}}_{g_k} \mathbf{F}_{g_1} \vec{\mathbf{h}}_{g_1}^H}{\vec{\mathbf{h}}_{g_1} \mathbf{F}_{g_1} (\sum_{j_i \in \mathcal{K}_{-g_{k+1}}} \vec{\mathbf{h}}_{j_i}^H \vec{\mathbf{h}}_{j_i} - \vec{\mathbf{h}}_{g_k}^H \vec{\mathbf{h}}_{g_k} + \frac{\sigma^2}{p_{g_k}} \mathbf{I}) \mathbf{F}_{g_1} \vec{\mathbf{h}}_{g_1}^H} \\
&= \upsilon_{g_k} / (1 - \upsilon_{g_k}) \\
&\overset{(d)}{\leq} \vec{\mathbf{h}}_{g_k} \mathbf{F}_{g_k} \vec{\mathbf{h}}_{g_k}^H \\
&\overset{(e)}{=} \delta'_{g,G} \mathrm{Tr}(\vec{\mathbf{R}}_{g_k,g_k} \mathbf{F}_{g_1}) \\
&+\delta_{g,G} \mathrm{Tr}(\vec{\mathbf{R}}_{g_k,g_k} (\sum_{j_i \in \mathcal{K}} \vec{\mathbf{h}}_{j_i}^H \vec{\mathbf{h}}_{j_i} + \frac{\sigma^2}{p_{g_k}} \mathbf{I})^{-1}) \\
&\overset{(f)}{=} \delta'_{g,G} \\
&\mathrm{Tr}(\vec{\mathbf{R}}_{g_k,g_k} (\sum_{j_i \in \mathcal{K}_{-g_1}} (\frac{M \Xi_{j_i} \mathbf{\Lambda}_G^{(G,G)}}{1+m_{j_i}} + \hat{\vec{\mathbf{h}}}_{j_i} \hat{\vec{\mathbf{h}}}_{j_i}^H) + \frac{\sigma^2}{p_{g_k}} \mathbf{I})^{-1}) \\
&+\delta_{g,G} \mathrm{Tr}(\vec{\mathbf{R}}_{g_k,g_k} (\sum_{j_i \in \mathcal{K}} (\frac{M \Xi_{j_i} \mathbf{\Lambda}_G^{(G,G)}}{1+m_{j_i}} + \hat{\vec{\mathbf{h}}}_{j_i} \hat{\vec{\mathbf{h}}}_{j_i}^H) + \frac{\sigma^2}{p_{g_k}} \mathbf{I})^{-1}) \\
&\overset{(g)}{=} \frac{\delta'_{g,G} M \alpha_{H,g_k} \rho_{H,g_k}}{\frac{\sigma^2}{p_{g_k}}} \\
&+ \frac{\delta_{g,G}(|\sqrt{\alpha_{H,g_k} \rho_{H,g_k}} + c_{g_k}|^2 + \Xi_{g_k}) + \delta'_{g,G}(c_{g_k}^H c_{g_k} + \Xi_{g_k})}{\sum_{j_i \in \mathcal{K}_{-g_1}} (\frac{\Xi_{j_i}}{1+m_{j_i}} + \delta'_{j,G} c_{j_i}^H c_{j_i}) + \eta + \frac{\sigma^2}{M p_{g_k}} - \zeta_g}
\end{aligned} \tag{A· 4}$$

where (d) come from the monotonically increasing function SLNR_{g_k} with respect to $\upsilon_{g_k} \in [0,1)$. Obviously, the optimal $\widetilde{\mathbf{w}}_g^{(opt)}$ can be obtained as $(\sum_{j_i \in \mathcal{K}_{-g_{k+1}}} \vec{\mathbf{h}}_{j_i}^H \vec{\mathbf{h}}_{j_i} + \frac{\sigma^2}{p_{g_k}}\mathbf{I})^{-1}\vec{\mathbf{h}}_{g_k}^H$ to maximize SLNR_{g_k}. We utilize the matrix inversion lemma in (25) and attain the maximum value of $\mathrm{SLNR}_{g_k} = \vec{\mathbf{h}}_{g_k}\mathbf{F}_{g_k}\vec{\mathbf{h}}_{g_k}^H$. And, (e) follows from the rank-1 perturbation lemma in [13], (f) follows the Theorem 1 in [13], (g) follows the Theorem 1 in [4].

Pingping Ji received the B.E. degree in communication engineering and the M.E. degree in communication and information system from the Nanjing University of Posts and Telecommunications, Nanjing, China, in 2014 and 2017, respectively. She is currently pursuing the Ph.D. degree with the School of Shanghai Jiao Tong University, Shanghai, China. Her research interests include multiple-in-multiple-out (MIMO) technology, reconfigurable intelligent surface (RIS), and precoding for massive MIMO.

Lingge Jiang received the B.E. degree in radio engineering from Southeast University, Nanjing, China, in 1982, and the M.E. degree in electrical engineering, and the Ph.D. degree in electronic system engineering from Tokushima University, Tokushima, Japan, in 1993 and 1996, respectively. In 1996, she joined the Department of Electronic Engineering, Shanghai Jiao Tong University, Shanghai, China. She is currently a Professor with Shanghai Jiao Tong University. She has authored or coauthored more than 170 journal and conference papers and has 59 awarded patents. Her current research interests include next generation wireless communication systems, wireless sensor networks, cognitive radio networks, cooperative communication, and intelligent information processing. She was the recipient of the 4th Nyoji Yokoyam Excellent Paper Award of Shanghai Jiao Tong University in 2000 and the Technique Invention Prize (second-class) of Shanghai Science and Technology Award in 2008 (20083041-2-R02).

Chen He received the B.E. and the M.E. degrees in electronic engineering from Southeast University of China, Nanjing, China, in 1982 and 1985 respectively, and the Ph.D. degree in electronics system from Tokushima University of Japan, Tokushima, Japan, in 1994. He was with the Department of Electronic Engineering, Southeast University of China, from 1985 to 1990. He joined the Department of Electronic Engineering, Shanghai Jiao Tong University of China, in 1996. He visited Tokushima University of Japan as a foreign researcher from October 1990 to September 1991 and visited the Communication Research Laboratory of Japan from December 1999 to December 2000 as a Research Fellow. He is currently a Professor with Shanghai Jiao Tong University, Shanghai, China. He has authored or coauthored more than 200 journal papers and more than 80 conference papers. His research activities focus on 5G wireless communication systems, including interference cancellation for multi-cells, wireless resource management, and cognitive radio. He received the Best Paper Award in the GLOBECOM 2007.

Di He Di He received the B.E. degree in information engineering from Huazhong University of Science and Technology, Wuhan, China, in 1996, the M.E. degree in communication and information engineering from Nanjing University of Posts and Telecommunications, Nanjing, China, in 1999, and the Ph.D. degree in circuits and systems from Shanghai Jiao Tong University, Shanghai, China, in 2002. From 2002 to 2004, he was a Postdoctoral Fellow with the Department of Electrical and Computer Engineering, University of Calgary, Canada. He is currently an Associate Professor with Shanghai Jiao Tong University. His research interests include wireless communications and wireless positioning.

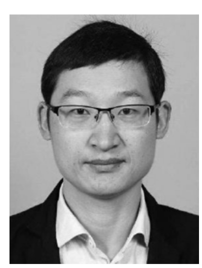

Zhuxian Lian received the B.E. degree in communication engineering from Information Engineering University, Zhengzhou, China, in 2011, and the Ph.D. degree from Department of Electronic Engineering, Shanghai Jiaotong University, Shanghai, China, in 2019. He is currently a Lecturer with the Jiangsu University of Science and Technology, Zhenjiang, China. His research interests include channel modeling, MIMO techniques, and precoding for massive MIMO.